2023 NA62 Status Report to the CERN SPSC

NA62 Collaboration

Abstract

The status of the NA62 experiment is reported. The current status of detectors and hardware is summarised, together with our experience of the 2022 data taking and plans for the 2023 data taking. The status of the $K^+ \to \pi^+ \nu\bar{\nu}$ analysis is presented, and highlights of rare and forbidden decay analyses and searches for exotic processes are discussed.

CERN-SPSC-2023-013 / SPSC-SR-326
26/04/2023

Contents

1 Introduction **3**

2 The 2022 run **4**

3 Status of the hardware and preparation for the 2023 run **7**

4 Data quality and processing **12**
4.1 Data quality monitoring system 12
4.2 The 2022 data: reprocessing, statistics, quality 12

5 Computing, software, and simulation **13**
5.1 Data volume, disk usage, expectation for 2023 13
5.2 Multi-thread reconstruction 13
5.3 Simulation improvements 14

6 $K^+ \to \pi^+ \nu\bar{\nu}$ analysis **14**
6.1 Selection improvements 14
6.2 Signal sensitivity 15
6.3 Background studies 15
6.4 Prospects and plans 17

7 Precision measurements of rare kaon decays **18**

8 Searches for exotic processes **20**

9 Publications **22**

References **22**

1 Introduction

After the completion of data taking in 2016–2018 (Run 1) and obtaining the first $> 3\sigma$ evidence for the $K^+ \to \pi^+\nu\bar{\nu}$ decay [1], NA62 restarted operations in 2021, took data in 2022, and is approved to run until LS3 (Run 2) [2]. The goals for Run 2 are: completion of the $K^+ \to \pi^+\nu\bar{\nu}$ branching ratio measurement as proposed [3]; measurements of flavour physics observables in the kaon sector; improvement of sensitivity to rare or forbidden decays of kaons; reaching the highest sensitivity to date in the searches for feebly-interacting particles predicted by several extensions of the Standard Model (SM).

Since the previous report in April 2022 [4], NA62 has taken data in 2022 for 215 days, with the beam at nominal intensity and an optimal quality of the spill for the most part of the run. The experiment has reached stable running conditions, with all the detectors working and a good efficiency of data acquisition (DAQ), especially in the second part of 2022 after a hardware readout issue in GTK was successfully fixed. Despite the higher beam intensity, the 2022 dataset is comparable to that of 2018, because about 25% fewer bursts were collected due to the 2022 run being two weeks shorter and hardware instabilities until mid-August affecting DAQ efficiency.

The 2022 data have been reprocessed with the full calibrations applied, and the $K^+ \to \pi^+\nu\bar{\nu}$ analysis is restarted with the main goal of improving signal efficiency with respect to Run 1, to properly handle new features related to the higher intensity, and to exploit the full power of the fourth station of the GTK and of a new veto counter.

Analysis of Run 1 data led to publication of new high-precision studies of $K^+ \to \pi^+\mu^+\mu^-$ [5], $K^+ \to \pi^0 e^+\nu\gamma$ [6] and $K^+ \to \pi^+\gamma\gamma$ [7] decays, and searches for forbidden decays [8]. Analysis of a dataset taken in 2021 in the beam dump configuration has produced the best result to date in the search for dark photon decays to two leptons [9]. Several analyses using Run 1 data are on-going, with results expected in 2023 both in the context of precision physics and direct searches.

A major upgrade of the core software has been released, with a multi-thread architecture of the reconstruction implemented allowing for a faster reprocessing. Continuous work is on-going to keep both the offline and online software up to date with the latest CERN-IT requirements. Finally, the NA62 simulation has been improved, with biasing methods developed to generate significant amounts of rare processes, including those responsible for the upstream background limiting the measurement of $K^+ \to \pi^+\nu\bar{\nu}$ decay in Run 1.

NA62 will restart data taking in May 2023. A major upgrade of the experiment in 2023 is the replacement of the CEDAR-N with the CEDAR-H. The 2023 period of data taking is expected to be 20–25% shorter than last year, due to CERN energy saving measures and compensation for the ion run in the North Area that was partially aborted in 2022.

The document is organised as follows: Section 2 summarises the 2022 run; Section 3 describes the main hardware activities that took place during the winter shutdown and the plans for the 2023 run; Section 4 describes the data quality monitor and reports about the status of the reprocessing of the 2022 data; the status of the software, computing and simulation is described in Section 5; the $K^+ \to \pi^+\nu\bar{\nu}$ analysis is reported in Section 6; Sections 7 and 8 summarise the status of the analyses of the kaon decays and exotic processes, respectively; and Section 9 lists the NA62 journal publications from May 2022 till April 2023.

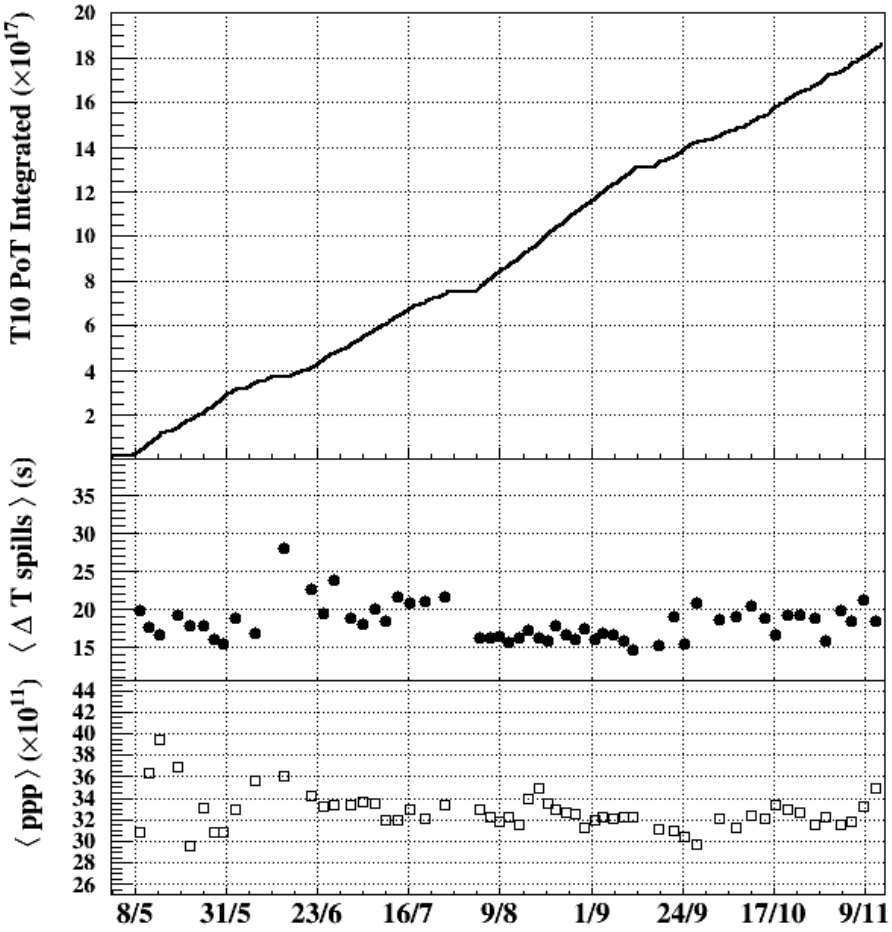

Figure 1: Characteristics of the beam delivered by the SPS to the T10 target in 2022 as a function of the time. Top: integrated protons on target. Middle: time interval between two consecutive spills averaged over about 10^4 spills. Bottom: intensity measured in proton-per-pulse from the T10 intensity monitor averaged over about 10^4 spills. Data reconstructed from TIMBER.

2 The 2022 run

The 2022 data taking was focused entirely on kaon physics, with the standard trigger configuration for $K^+ \to \pi^+\nu\bar{\nu}$ and rare and precision decays. In the last part of the data taking, some tests for hardware upgrades in preparation for the 2023 run were performed. Overall, beam and detectors performed smoothly, with the exception of beam instabilities in the first month of the run and GTK readout issues until August. Below is a list of the most relevant features of the 2022 data taking period.

Beam
Following the secondary beam tuning in the P42 and K12 lines, the SPS experienced extraction problems at the beginning of the run due to water leaks, which forced several days of beam downtime. The run restarted in mid-May at a nominal beam intensity. In total, the SPS has delivered 1.8×10^{18} protons on the T10 target (PoT) integrated over the whole data taking period (Figure 1, top). The average time difference between two consecutive bursts was about 18.2 s,

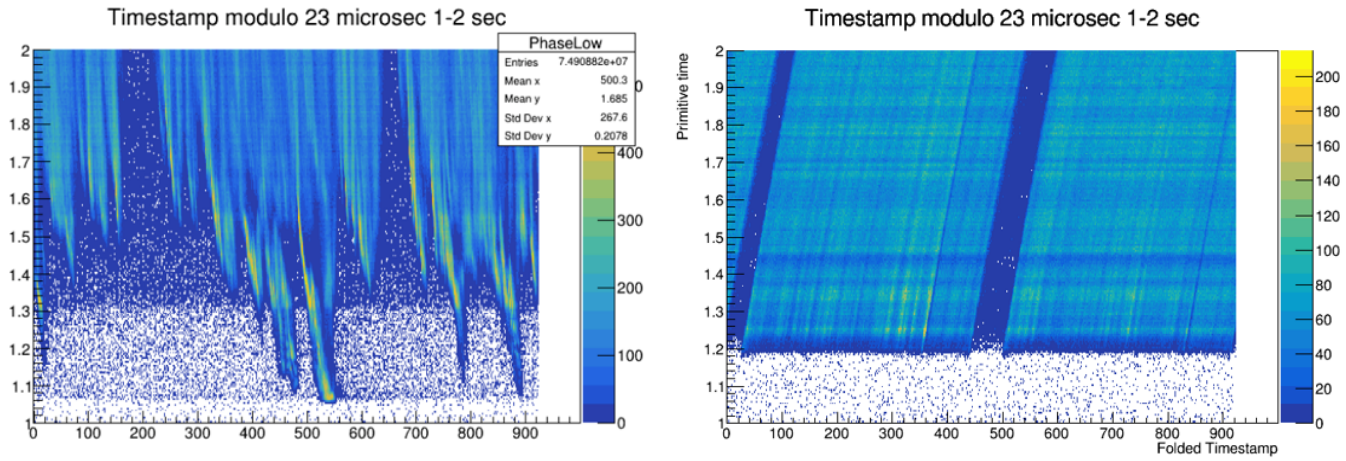

Figure 2: Timestamp modulo SPS revolution time. Left: the 2021 data exhibits "flares" in the first second of the extraction. Right: the 2022 data have a smooth beam profile.

corresponding to an average duty-cycle of 0.25. The actual time between consecutive spills varied during the run from 14.4 s to 20–25 s, depending on the activities in parallel to the SFTPRO cycle, like, for example LHC filling, Awake run, or beam tests (Figure 1, middle). The average intensity on T10 of 32.5×10^{11} protons per pulse (ppp) was quite stable during the run, except for the initial setup period and the last days of run when the intensity increased to 35×10^{11} ppp (Figure 1, bottom). These values are the average over 10^4 bursts, corresponding to about 5 days of data taking. Fluctuations of the order of 10% in the T10 intensity were observed on a daily basis. The corresponding average intensity on T4 was 70.5×10^{11} ppp, with values varying by up to $\pm 5 \times 10^{11}$ ppp depending on the period. The beam steering suffered from focusing issues on T4 that led to lower transmission to T10 than expected. This problem, also present in 2021, is now understood to be due to a badly misaligned vacuum chamber just downstream to T4 target. The chamber has now been removed.

The spill problems affecting the 2021 data have been solved thanks to close collaboration with the BE-OP and SY-RF groups that found an issue in the radiofrequency (RF) voltage settings at extraction. The flares of intensity observed in the first 1–1.5 seconds of the spill in 2021 were then cured before the start of the 2022 run, and the spill structure appeared smooth throughout the spill for the entire period of data taking (Figure 2). Nevertheless, keeping such a spill required a careful monitoring and tuning of the extraction conditions by the SPS operators, which will also be required for the 2023 run. Beam intensity spikes are particularly harmful for NA62, leading to dangerous hardware instabilities and jeopardizing the data quality as in 2021.

NA62 data taking performance

The 2022 data taking performance obtained from an analysis of SPS spills recorded by the NA62 run control is summarised in Table 1. The T4 availability is the fraction of spills recorded with beam on T4 with respect to the expected number of spills. The T10 availability is the fraction of spills recorded with beam on T10 and T4 with respect to the spills with beam on T4, and quantifies the amounts of issues with the beam line and to the NA62 detectors that required access to the cavern. The NA62 availability is the fraction of spills written on disk compared to the spills recorded with T10 and T4 on. In this case missing spills are due to hardware problems being fixed without stopping the beam on T10. The trigger efficiency is the fraction of events collected compared to the total number of events that should have been collected, averaged over

Table 1: Summary of the 2022 data taking compared to that of 2021. Columns 2 to 5 are the T4 and T10 availability, the NA62 availability, and trigger efficiency. The last column is the product of the entries of columns 2 to 5.

Period	T4	T10	NA62	Trigger	Total
2022	0.753	0.906	0.844	0.856	0.493
2022 ($>$ 10/08)	0.775	0.924	0.877	0.904	0.568
2022 ($<$ 10/08)	0.726	0.883	0.800	0.795	0.408
2021	0.710	0.871	0.800	0.731	0.362

10^3 spills. The 2022 trigger efficiency is the result of 0.916 trigger efficiency at L0 and 0.934 at L1. The inefficiency is mainly due to missing primitives and trigger generation because of choke signals at L0, and GTK and LKr not sending data at L1. The product of the NA62 availability and trigger efficiency is a figure of merit for the NA62 data taking efficiency, which amounted to 72.2% in 2022. The last column in Table 1 is the product of the previous efficiencies and quantifies the fraction of the data taking period in which NA62 wrote data on disk. The poor performance in 2021 was mainly due to the spill issues causing TDAQ instabilities, leading to a data taking efficiency below 60%. In 2022 the performance significantly improved after the 10/08/2022 when a problem in the GTK optical connection was found and fixed. After this date the NA62 data taking efficiency increased from 63.6% to 79.3%, reaching a performance in line with that of the 2018 data taking, in which, however, the intensity was about $\times 1.4$ lower.

GTK
In the first part of the run the GTK readout experienced frequent blocks, often causing loss of several spills to restart it. Various improvements on the software side allowed a partial mitigation of the instabilities. However, a major readout problem identified in August was related to a hardware issue of the optical splitter for the control and clock signals. Once fixed, the detector readout worked smoothly for the rest of the data taking.

LKr
The firmware of the LKr readout boards was updated at the beginning of the 2022 run and thoroughly tested. Its performance related to the event packing has been improved to optimise operation at nominal intensity. Typical problems with faulty modules were cured using a substantial spare supply, which is continuously kept up-to-date.

Vetocounter
New CFDs were installed, allowing the the detector to run with optimal threshold levels. The detection efficiency of the vetocounter was measured to be better than 95% for all the slabs. The TEL62 was still the main readout of the vetocounter during the 2022 run, with the new TDC-Felix readout running in parallel. Eventually a working TDC-Felix firmware configuration was deployed at the end of the run allowing collection of data with both readouts for offline comparison.

Trigger and L0TP+
The trigger chain operated smoothly in 2022. The CHOKE signals were activated for all the detectors with a CHOKE line. The L0 trigger processor board (L0TP) operational since 2015 was still in use to combine the primitives and deliver the L0 trigger decision. The average L0

rate at nominal intensity was about 1 MHz. The number of L0 triggers was stable with intensity throughout the run. The data acquisition system for the trigger primitives, used for monitoring purposes, was disabled in 2021 because of L0 trigger instabilities introduced by the latency of the Ethernet switch that duplicated the primitives. The system was once again fully operational in 2022 thanks to the use of the Ethernet TAP that allowed the duplication of the primitives with zero latency.

A new L0 Trigger Processor (L0TP+) was designed and built in 2021 with a two-fold purpose: firstly, to allow the implementation of more complex trigger lines by using a more powerful FPGA; secondly, to overcome the old architecture of the Gigabit output connection of the present L0TP limiting the amount of data that can be sent to the PC farm. At the end of the 2022 run the L0TP+ was tested during data taking at nominal intensity. The test focused on the definition and implementation of the connection protocol between the L0TP+ board, the Run Control and the PC farm, the generation of physics and calibration triggers, the processing of choke signals, and the handling of the SPS signals. The test was successful except for a cross-talk problem in the cable used to send the start- and end-of-burst signals, affecting the generation of physics triggers.

The L1 trigger algorithms were improved to reduce the downscaling factors of the rare decay trigger lines (Section 7). All rare decay trigger lines were operational for the whole run.

CEDAR-H test beam

The CEDAR counters designed at CERN utilise a variable-aperture diaphragm with fixed central diameter to distinguish beam particles, as different particle types produces a Cherenkov ring of different radius when passing through a gas radiator. The NA62 CEDAR (CEDAR-W) operates with Nitrogen gas (N_2) as the Cherenkov radiator, which contributes $3.5 \times 10^{-2} X_0$ of material in the beamline. The amount of material can be reduced to $3.2 \times 10^{-3} X_0$ by replacing the Nitrogen with Hydrogen (H_2). To this end, a second CEDAR was modified for use with H_2 in 2021–2022 [10].

In October 2022, we carried out a test in the H6 beamline at CERN was to measure the performance of the modified CEDAR (CEDAR-H). The test beam demonstrated that the CEDAR-H satisfies the three main criteria for operation at NA62 [11]. Firstly, the CEDAR-H was successfully aligned in the H6 beamline, validating the new optical system and its alignment inside the CEDAR vessel. Secondly, pressure scans made with a large aperture showed that the CEDAR-H is 99% efficient in detecting particles, indicating excellent performance of the counter. Finally, pressure scans made at smaller apertures showed that CEDAR-H meets NA62 requirements on the separation of kaons and pions in the beam.

Following the successful test beam, CEDAR-H was installed on the NA62 beamline for the data taking in 2023.

3 Status of the hardware and preparation for the 2023 run

The main activities during the winter shutdown were the installation of the new CEDAR-H and the commissioning of the L0TP+. Issues identified during the 2022 run have been investigated and fixed, and all detectors have undergone routine maintenance without significant upgrades for the 2023 run.

KTAG

The CEDAR-W detector was replaced with CEDAR-H in February 2023 (Figure 3). This required dismounting the KTAG detector hosting the photon collection and detection systems, removing CEDAR-W, installation of CEDAR-H, and re-mounting of the KTAG (Figure 4). This all proceeded as planned. New spherical mirrors for the KTAG were coated, mounted, and aligned by experts at CERN. After the installation, the KTAG front-end and readout electronics were tested and found to be fully operational.

The CEDAR-H was subsequently connected to the gas distribution system. Leak tests and full commissioning of the Gas Control System (GCS) with nitrogen have been successfully completed. A filling with H_2 gas has been performed by GCS and KTAG experts to verify the procedure prior to the start of data taking. Various developments related to flammable-gas safety requirements have been completed. Examples are: a pavilion was erected to be used as the basis of a flammable gas detection system at both CEDAR ends; an isolation box was constructed to separate the motors from a potential H_2 leak; connectors inside the ATEX zones around the CEDAR were removed, which required the replacement of several temperature sensors with ATEX-rated devices; and the grounding of all metal items close to ATEX zones has been implemented. The CEDAR alignment and diaphragm motor controls fully tested and are working.

An ATEX-rated pump was to be procured to remove H_2 from the CEDAR at the end of yearly data taking, and a new exhaust system with larger-diameter piping was to be installed. However, due to lack of personnel and hardware, these two aspects of the system are delayed until next year. Instead, the H_2 will be removed from the CEDAR by flushing with N_2 over a period of 10–12 hours. This method was utilised successfully during the 2022 test beam.

A safety protocol detailing all operational and emergency procedures has been produced. This includes a section for shifters that specifies actions to be taken in an emergency, included in the NA62 shifter training. The CEDAR-H passed the HSE inspection at the end of April and is ready to be used in NA62 from 2023 onward.

The CEDAR-H project was successful as due to the collaboration between NA62 and several CERN groups. We would like to thank the following CERN groups for their contribution and support during team beam and installation on NA62 beamline: BE-EA, SY-BI-PM, SY-BI-XEI, EP-DT-FS, EP-DT-EF, EN-MME, HSE-OHS, HSE-FRS, EN-EL-EWS, EN-AA, BE-CEM, EP-DI-SO, BE-ASR-SU, BE-ICS.

GTK

Investigation of the GTK readout hardware revealed a fault in the propagation of the clock and reset signals, causing the instabilities that were temporarily fixed during the 2022 run. In January–March 2023, all relevant connectors were cleaned, the problematic optical splitter was identified and replaced. Note that the GTK readout instabilities were not present in Run 1 because this splitter was installed in LS2 together with the modifications of the GTK to accommodate the fourth station. New delay fibers with improved connectors were installed during the 2023 shutdown, and a fine-tuning of the relative timing of the GTK stations performed. Signal and configuration fibers of station 0 were replaced with longer ones to reduce the stress on the connectors.

Vetocounter and CHANTI

The new TDC-Felix readout boards installed on the Vetocounter were successfully commissioned in 2022. The data taken with both the new and the TEL62 readout were analyzed offline showing equal, or better performance of the new readout system, especially at higher rates. The new TDCs have been found to be sensitive to neutrons in the beam halo, so the rack was displaced

Figure 3: Top: The CEDAR detector is positioned in a Grey room at CERN; then the internal optics is extracted from the vessel to be replaced with new components. Bottom: The CEDAR with optics optimised for H_2 is installed on the NA62 beam line; the KTAG detector (hosting photon collection and detection systems) is then mounted on the upstream end. The blue plastic surrounding the CEDAR nose protected the quartz windows during transportation.

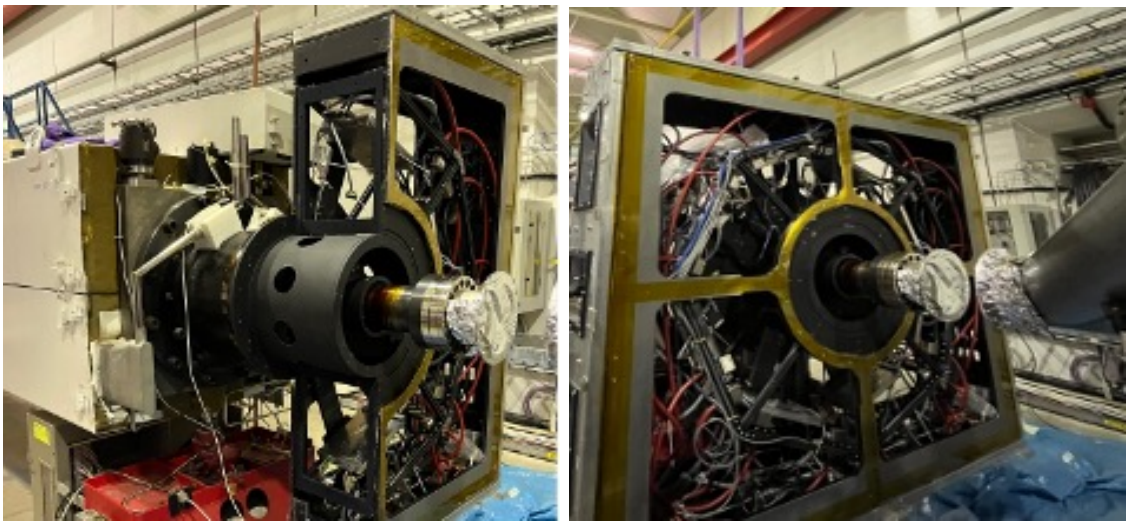

Figure 4: Left: Half KTAG (Saleve-side) mounted on the CEDAR, the frame is positioned on the ATEX cylinder support around the CEDAR nose, and bolted to a flange at the downstream end of the cylinder. Right: Both Saleve and Jura KTAG halves mounted on the CEDAR, the internal frame for positioning of the light boxes with PMTs radially around the CEDAR nose is visible.

and additional shielding was installed. A detailed calibration of the detector using muons will be performed at the beginning of 2023 data-taking. All the CHANTI SiPMs were replaced during the winter shutdown because of the high dark current of the old ones. We plan to use the new TDC-Felix boards to read out the CHANTI, as with the Vetocounter. To validate the new CHANTI readout, a special splitter board has been prepared to connect a fraction of CHANTI channels to the new readout in parallel with the TEL62-based readout. Once validated, the new readout will replace the TEL62 boards.

STRAW, RICH, NewCHOD

The STRAW detector and readout system were stable throughout the 2022 run, and are ready to take data in 2023. A problem with a RICH mirror piezomotor has been fixed. The mirror alignment will be checked at the beginning of the 2023 run. The NewCHOD SiPMs in the inner region have been replaced. An inspection of all the optical connections between fibers and SiPMs showed non-uniform distribution of optical grease, which has been fixed.

LAV, LKr, IRC-SAC

The LAV system was checked in March 2023, and it is fully operational. A few LKr channels with peculiar behaviour have been investigated. The replacement of the corresponding transceiver did not fix the problem, suggesting a possible issue inside of the cryostat. In any case, NA62 can safely operate with those faulty channels in the LKr without degradation of the performance. The standard IRC-SAC readout is ready. A parasitic additional readout, based on 250 MHz FADCs in a Gandalf system, is under installation. The goal is to study the behaviour of fast digitised waveforms in a real experimental environment in preparation for the HIKE proposal.

MUV1,2,3 and HASC

Several faulty MUV1 and MUV2 photomultipliers have been replaced. All the MUV3 channels have been checked with cosmic rays and once the beam was partially available at the end of April, muons. A broken channel in the HASC, already faulty in 2022, has been replaced.

New TDC, trigger, PC farm

The firmware with a 390 ps digitisation step is implemented on the new TDC of the Vetocounter and CHANTI. A version of the firmware with a 100 ps digitisation step is under development and will be deployed and tested during the 2023 run.

The L0TP+ operational problems observed during the 2022 test were fixed in the winter shutdown. The new board has been fully commissioned and integrated into the NA62 readout system. The L0TP+ is now ready to be used for the run, fully replacing the L0TP that had been operating since 2015.

An investigation into the bad behaviour of several LKrL0 trigger boards has been performed. The firmware for the LKrL0 data readout has been debugged, and will be online for the 2023 run. Additional work has been done to speed up LKrL0 initialisation and startup. Further work is in progress to implement a di-electron trigger based on the calorimeter information.

New L1 trigger algorithms have been developed based on data from the LAV and RICH detectors. These algorithms exploit the correlations between tracks reconstructed in the STRAW and signals in the detectors downstream, aiming to fully exploit the information available at L1. The upgraded LAV algorithm reduces the random veto by ignoring hits upstream of the decay vertex, and by applying slewing-corrections to improve the time-resolution which allows tighter cuts (thus a less stringent veto) to be used. The new RICH algorithm projects negatively charged STRAW tracks to the RICH, and checks the RICH data for a corresponding electron signature.

During the 2022 run, a new merger PC ("merger 4") was often disabled from data taking because of an operational issue. Investigations have allowed the problem to be isolated to the RAID controller and fixed. Sixteen new additional PCs have been purchased, delivered at the end of March, and will gradually replace the existing farm nodes. The network package DPDK has been successfully tested with the farm software and will be used for the operation of the farm.

Additional PDU connections have been deployed to be able to remotely switch on/off more critical equipment, as well as recently installed network switches.

Plans for the 2023 run

The beam tuning started in mid-April. The faulty vacuum chamber in T4 was removed and the beam profiles at T10 now confirm that the transmission problems between T4 and T10 are fixed. While the beam tuning has been done in the second half of April and is almost completed, the first two weeks of the 2023 data taking are allocated for detector setup. The startup period could be a few days longer than usual because of the commissioning of the new CEDAR-H and L0TP+. Note that the pressure scan and alignment procedures of the CEDAR-H are the same as those of the CEDAR-W, routinely performed at the beginning of every run since 2015.

NA62 will run in 2023 mostly for kaon physics at the nominal beam intensity with spill quality control as in 2022. Some periods at 60–70% of nominal intensity could take place to study systematic effects, backgrounds and overall efficiency related to the $K^+ \to \pi^+\nu\bar{\nu}$ analysis. A period of about 10 days in the dump mode at $\times 1.5$ nominal intensity, as in 2021, is expected. The exact dates are to be defined later.

4 Data quality and processing

4.1 Data quality monitoring system

The quality of the data of NA62 relies on the online data quality monitoring system. This system is organised in three levels.

1. *Fast Processing* is meant to provide histograms in the Control Room and on the web for almost real-time monitoring. As soon as a spill is collected, a subset of data taken by a minimum bias trigger is processed using the standard offline reconstruction software. A dedicated PC dispatches the histograms. The time from taking data to displaying the histograms depends on the instantaneous intensity, and was about two minutes in 2022.

2. *Fast Post-Processing*; takes place at the end of a run[1], and provides a monitoring tool for detector experts on a daily basis, with larger statistics than the first level. This step makes use of the output files from the fast processing, therefore the delay time depends only on the length of a run.

3. *Prompt Processing* relies on the offline processing of all the data from the raw files temporary stored on EOS. This level performs the full detector calibrations, filters the data and runs several analysis routines. The delay time is typically several days, and is sensitive to possible configuration changes that may occur during data taking, halting the prompt processing of the whole run if not propagated to the software quickly enough.

During the 2022 run, about 85% of the spills were fully processed by the prompt processing, which was a significant improvement on 2021. Moreover, there was a sizable reduction of the Fast Processing time, thanks to a new system of receiving the data directly from the farm nodes instead of the merger PCs, and the improved spill quality. In 2023 we expect a further reduction of the processing time using a new reconstruction software in multi-thread mode (Section 5.2). The PC displaying the Online Monitor plots in Control Room was replaced during the winter shutdown. The new machine supports AlmaLinux9, forcing a transition of the entire NA62 framework to this new CERN-supported operating system.

4.2 The 2022 data: reprocessing, statistics, quality

The 2022 data taking ended in November, and all the data were centrally reprocessed by March 2023. The reprocessing software runs dedicated data-quality routines for each subsystem, to identify which bursts are "bad" and must be excluded from the physics analyses. The full 2022 data sample is split into five subsamples (A, B, C, D, E, in chronological order) according to the main features of the data taking; the data quality is almost uniform within each subsample.

The 2022 data sample consists of 4.03×10^5 SPS spills. For comparison, the numbers of spills are 1.45×10^5 in 2021 and 5.25×10^5 in 2018. The smaller number of spills in 2022 than in 2018 is due to a 15 days shorter run, and GTK readout instabilities in the first part of the run.

About 20% of the collected spills are flagged as bad and excluded from the $K^+ \to \pi^+\nu\bar{\nu}$ analysis. The sources of bad bursts are: issues in one or more subsystems used in the $K^+ \to \pi^+\nu\bar{\nu}$

[1] A "run" is defined as a collection of about 1500 consecutive spills equivalent to about 6 hours of data taking with the shortest SPS duty cycle. Shorter runs are taken in case of external factors forcing the stop of the data acquisition.

analysis; the spills collected with trigger conditions not appropriate for the $K^+ \to \pi^+\nu\bar{\nu}$ analysis; or non-recoverable processing failures. A high fraction of bad spills is found in sample A and a part of sample C, due to hardware problems in the Small Angle Veto and VetoCounter subsystems. The fraction of bad spills in the other samples is about 10%, in line with the 2018 run. The $K^+ \to \pi^+\nu\bar{\nu}$ analysis has the largest fraction of bad spills as it makes use of all the subdetectors. Some of the bad spills are usable in other physics analyses that do not rely on the information coming from all subsystems. Studies to recover part of the bad spills for the $K^+ \to \pi^+\nu\bar{\nu}$ analysis are ongoing.

No relevant remaining data quality issues are found for the data collected in 2022 and declared good for the $K^+ \to \pi^+\nu\bar{\nu}$ analysis.

5 Computing, software, and simulation

5.1 Data volume, disk usage, expectation for 2023

A total of 2.7 PByte of raw data were taken and written to CTA in 2022. At this moment, the total amount of NA62 data on CTA (accumulated since 2012) is about 12.9 PBytes, of which 75% is raw data.

After processing and filtering, NA62 data are kept on EOS for individual user analyses. The projection done in 2020 based on 2018 data estimated a yearly increase of about 1 PByte. Due to the larger than expected size of the 2021 data, additional storage (2 PByte) was requested and granted in summer 2022. Additionally, the NA62 normal yearly allocation of 1 PByte was granted in April 2023. At the moment the total quota is 9.4 PByte, of which 200 TByte are reserved for online usage (raw data to CTA and prompt processing).

We would like to express our gratitude to the IT Department for their support and expertise in assisting the needs of the experiment, and in particular to Xavier Espinal and Bernd Panzer-Steindel, for the excellent support and services provided to us.

5.2 Multi-thread reconstruction

The Fast Processing monitoring is performed by running the full reconstruction for each spill acquired, using only events accepted by the control trigger and largely downscaled. Four powerful computers are used to run the reconstruction process on several spills in parallel (up to 16 per computer). The file produced is stored in a common NFS area, picked up and displayed by the online monitor software for fast feedback. While the delay between the acquisition and display of a spill was on average 2 minutes in 2022, it could reach up to 10 minutes, which is too slow for real-time feedback. In addition, the large downscaling required to reduce the processing time results in low event numbers in the histograms for detectors with low occupancy.

To improve the situation, the core of the NA62 reconstruction software was entirely rewritten in 2022 and is now ready to be used in the data-taking. Several bottlenecks and inefficient programming patterns have been identified and improved, resulting in a CPU usage reduction of a factor 4 for TEL62-based detectors. The data flow has also been rewritten from scratch, resulting in increased flexibility for future developments, and resolving unsatisfactory patches applied over the years to add features not present in the previous architecture. The new data flow also allows the usage of the software in multi-threaded mode, using a multi-stage producer-consumer pattern. This new mode will be used in the online monitoring system to increase the processing speed, thus reducing the delay between data acquisition and display. The downscaling will also be re-adjusted

to obtain an acceptable trade-off between the delay and the number of events reconstructed to increase the statistics for low occupancy detectors.

5.3 Simulation improvements

Significant efforts were made over the last year to enhance the functionality of the NA62MC simulation framework. A flexible placement and configuration scheme for beamline elements and detectors has been introduced, which allows switching between Run 1 and Run 2 configurations and facilitates exploratory studies related to the possible future developments of the NA62 programme. The 2022 running conditions have been incorporated in the simulation. New event biasing schemes introduced at generation level are instrumental for the elucidation of the background mechanisms to the $K^+ \to \pi^+\nu\bar{\nu}$ decay, in particular from the major $K^+ \to \pi^+\pi^+\pi^-$ and $K^+ \to \pi^+\pi^0$ decays upstream of the decay region followed inelastic π^+ scattering. The decay generator library has been routinely developed to support the on-going rare kaon decay analyses, the beam-dump programme, and exploratory studies.

The NA62MC has been successfully migrated to a recent version of GEANT4 (v11). This work is part of the ongoing effort to migrate the entire NA62 software framework to a newer LCG version (LCG102). Extensive validation studies were conducted in the first part of 2023, and the framework now supports the use of GEANT4 v11.0.3. This change is expecrted to improve the agreement between data and simulations in terms of the description of electromagnetic shower shapes and energy deposits.

6 $K^+ \to \pi^+\nu\bar{\nu}$ analysis

6.1 Selection improvements

The study of the $K^+ \to \pi^+\nu\bar{\nu}$ decay with Run 2 (2021–2022) data is progressing and has reached an advanced stage. Building on the firm Run 1 foundation [1], the analysis has been re-optimised for the higher intensity working point and multiple improvements have been implemented. Some of these are briefly described below.

- The new Run 2 detectors have been fully integrated into the analysis. Firstly, the use of the 4^{th} GTK station increases reconstruction efficiency by about 3%. Secondly, the Vetocounter reduces the critical upstream background by providing a powerful veto of in-time decays in the upstream region. Thirdly, using the HASC2 to veto additional particles has reduced the $K^+ \to \pi^+\pi^0$ and $K^+ \to \pi^+\pi^+\pi^-$ backgrounds.

- Photon veto conditions are improved, in particular for the LKr calorimeter where an updated reconstruction algorithm has been developed, reducing the random veto.

- Selection criteria relating to rejection of additional activity have been overhauled and re-tuned for higher intensities.

- The allowed volume for vertex reconstruction has been re-optimised, gaining signal acceptance and reducing background contamination.

6.2 Signal sensitivity

The effective signal acceptance has been improved with respect to the Run 1 analysis as the result of improvements in the selection acceptance by at least 20% in relative terms, at the same level of random veto efficiency (approximately 65%) despite the intensity increase. The overall effective signal efficiency is defined as the product of the selection acceptance for MC simulations with no pileup, $A_{\pi\nu\bar{\nu}}$, and the random veto efficiency, ε_{RV}, which accounts for losses due to additional accidental activity in events. The effective signal efficiency is shown in Figure 5, comparing the published analysis of 2018 data [1] and the current analysis of 2022 data. The average instantaneous intensity has increased from 400 MHz in 2018 to 580 MHz in 2022[2], and selection improvements have nevertheless allowed an increase in effective signal efficiency.

A preliminary evaluation of the number of expected SM $K^+ \to \pi^+\nu\bar{\nu}$ events for the 2022 dataset alone gives $N_{\pi\nu\bar{\nu}}^{SM,exp} = 8.0 \pm 0.4 \pm 1.0_{\text{ext}}$, where the first uncertainty is primarily systematic and the second is due to the SM branching ratio. The systematic uncertainty quoted is an indicative figure from preliminary studies; a detailed evaluation is underway. The mean number of expected SM $K^+ \to \pi^+\nu\bar{\nu}$ events per good SPS spill is approximately 2.5×10^{-5}. Compared to the equivalent figure for the Run 1 analysis this value represents an improvement by approximately 60%. The increase is partly due to selection changes described above, and partly due to the increase in beam intensity for the 2022 data. If the improved analysis were applied also to Run 1 data, the mean number of expected signal events per burst would be greater in Run 2 wrt Run 1 data by approximately 10%. This is the result of a larger kaon rate, convoluted with lower efficiency due to the corresponding additional activity. Therefore, by operating the experiment at the higher-intensity working point, as in 2022, the signal yield slightly increases with respect to Run 1. The analysis optimisation is still in progress and, anyway, running at nominal intensity gives additional margin to further improve the signal yield.

The combined 2021 and 2022 dataset is being studied. The overall number of expected signal events is approximately 10. With data-taking efficiency and data quality control improving year-on-year (Sections 2 and 4), it is expected that in a nominal year of data taking there is further room for improvement on the current status.

6.3 Background studies

Detailed background studies are ongoing, and are at an advanced stage. For kaon-decay backgrounds, despite selection changes to improve signal acceptance and the significant intensity increase, the relative background contributions have been maintained at the same level as Run 1. Figure 5 (right) shows the events remaining in the background regions, used for background evaluation, after the signal selection is applied to the 2022 dataset. Table 2 shows a comparison of the expected number of signal and background events between the published analysis of 2018 data and the current status of the analysis of 2022 data. Evaluation of the upstream background is ongoing and is discussed below.

With the inclusion of the new Vetocounter in the analysis, and the modified K-π matching scheme including the 4$^{\text{th}}$ GTK station, a new procedure to evaluate the upstream background is being explored. By exploiting the information from the Vetocounter it has been demonstrated that specific upstream background mechanisms involving upstream decays of $K^+ \to \pi^+\pi^0$ and $K^+ \to \pi^+\pi^+\pi^-$ can be suppressed by a factor of more than three. This is illustrated in Figure 6

[2]The rate in 2022 is consistent with the definition of nominal intensity, as the effective spill length was about 4 s. Previous estimates of nominal intensity corresponding to 750 MHz assumed 3 s effective spill length.

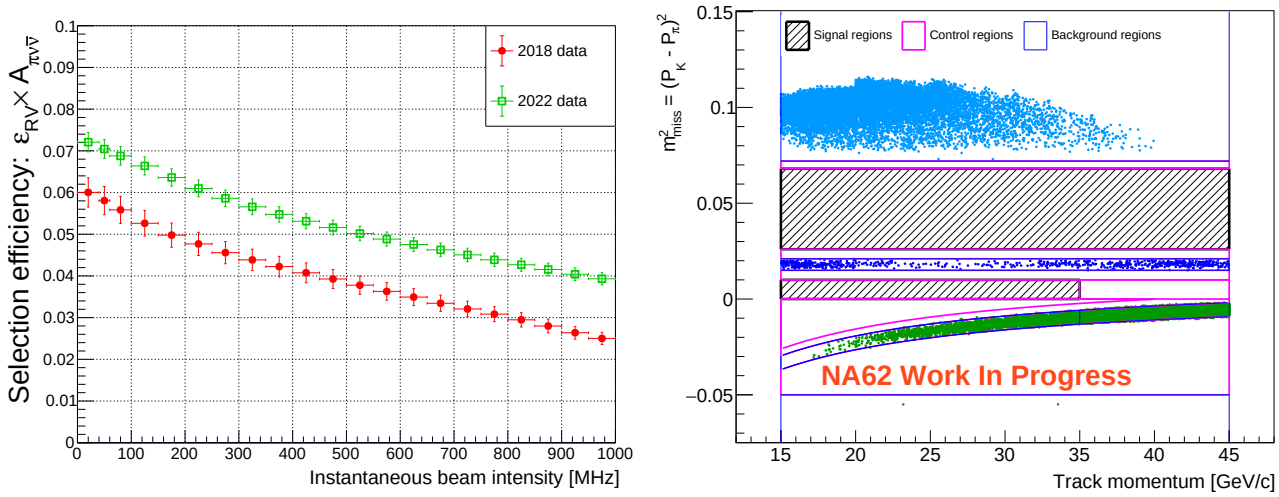

Figure 5: Left: comparison of effective selection efficiency, i.e. the product of MC selection acceptance and the random veto efficiency, as a function of instantaneous beam intensity for 2018 and 2022 data with the old and new analysis strategies, respectively. Right: number of events from the 2022 dataset passing the signal selection. The signal and control regions are kept masked so only the background regions are displayed, with the light blue, dark blue and green points indicating events in the regions dominated by $K^+ \to \pi^+\pi^+\pi^-$, $K^+ \to \pi^+\pi^0$ and $K^+ \to \mu^+\nu$ decays, respectively.

Table 2: Comparison between numbers of expected signal and background events in the 2018 and 2022 datasets. Numbers presented for 2018 are as published in [1], using the Run 1 analysis, while those for 2022 are using the current state-of-the-art analysis. The number of good bursts in 2022 data is approximately 70% of the number in 2018 data (Section 4.2).

Process	Expected number of events in signal regions	
	2018	2022
$K^+ \to \pi^+\pi^0$	0.75 ± 0.05	0.82 ± 0.03
$K^+ \to \mu^+\nu$	0.64 ± 0.08	0.74 ± 0.06
$K^+ \to \pi^+\pi^+\pi^-$	0.22 ± 0.08	0.09 ± 0.02
$K^+ \to \pi^+\pi^-e^+\nu$	0.51 ± 0.10	0.31 ± 0.16
Upstream	$3.30^{+0.98}_{-0.73}$	WIP
$K^+ \to \pi^+\nu\bar{\nu}$	7.58 ± 0.85	8.0 ± 1.1

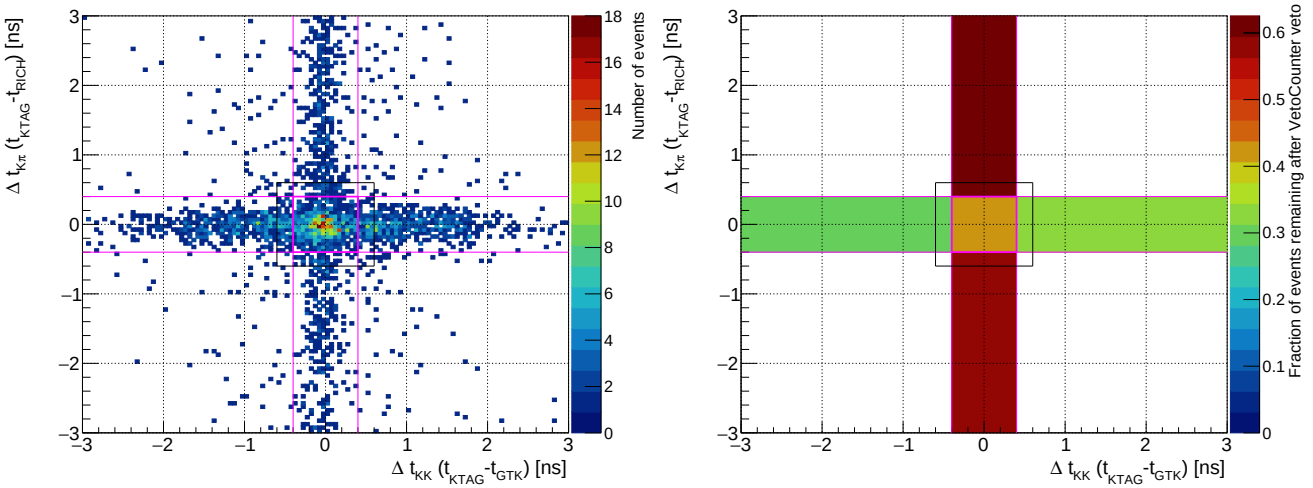

Figure 6: Left: number of events in a control sample enhanced of upstream-background-like events as a function of the time differences between the KTAG, GTK and RICH detectors. Right: fraction of these events remaining after the application of the VetoCounter veto criteria, displayed as an integral for the vertical and horizontal arms and their overlap region, as indicated by the magenta lines. The black square indicates the region selected in the main analysis.

where the left panel shows the distribution of a sample enhanced with upstream-background-like events, and before applying the Vetocounter criteria, in a two-dimensional plane of time-differences $t_{GTK} - t_{RICH}$ versus $t_{KTAG} - t_{GTK}$. In this plane background arising from upstream decays, plus accidental matching to a pileup GTK track, populates the horizontal band where the KTAG and RICH times match. This is because the K^+ detected by the KTAG matches the particle detected in the RICH downstream. Meanwhile the KTAG and GTK times do not match since the GTK track associated with the event is an accidental track and not the one associated to the K^+ detected by the KTAG. In Figure 6 the fraction of events remaining after the Vetocounter criteria is applied is shown integrated for the upper and lower horizontal and vertical arms, and the central overlap region. For the horizontal arms, dominated by upstream decays, the fraction of events after the Vetocounter is approximately 30%, corresponding to a rejection factor of just over 3. In the vertical arms the Vetocounter does not reduce the number of events by as much, since this region is not dominated by the upstream decays the Vetocounter was designed to detect. In the overlap region at the centre, where there is a mixture of the two populations, the Vetocounter rejection factor is consistent with the expected proportions of the two populations.

6.4 Prospects and plans

Further improvements to the selection are under study. A more aggressive approach to increasing signal acceptance has resulted in control samples used to evaluate the upstream background becoming contaminated with other, unrelated, events. Investigations are in progress to determine if the contamination can be removed or an alternative strategy can be adopted to evaluate the upstream background. Improvements in the treatment of accidental activity are under development, including machine learning techniques. The particle identification strategy using the calorimeters is also being reviewed; a new set of criteria using a convolutional neural network classifier is being evaluated. The procedure of matching the downstream STRAW track to an upstream GTK track is being examined in detail, and alternative techniques are being evaluated.

Using Run 2 data taken so far (2021–2022), an improved sensitivity for the measurement of the branching ratio of the SM $K^+ \to \pi^+\nu\bar{\nu}$ decay is anticipated. The analysis strategy, signal expectation and background predictions are being finalised for the analysis of 2021–2022 data. In addition, work is ongoing for further analysis improvements, including further holistic optimisations for high-intensity conditions.

7 Precision measurements of rare kaon decays

A broad rare decay programme is enabled by auxiliary prescaled multi-track and minimum-bias trigger chains operating along with the main $K^+ \to \pi^+\nu\bar{\nu}$ trigger. The L0 trigger lines for collection of K^+ decays to lepton pairs established in 2016 are based on RICH and CHOD multiplicity requirements, the total energy deposited in the LKr and MUV3 signal multiplicity conditions. The L1 trigger conditions involve beam kaon identification by the KTAG and fast reconstruction of a negatively charged track in the STRAW spectrometer. The Run 1 (2016–2018) dataset is equivalent to 10^{12} kaon decays to di-electrons, 3×10^{12} decays to di-muons, and 10^{12} decays to electron-muon pairs. The Run 1 dataset collected with generic multi-track and minimum-bias trigger conditions is equivalent to about 10^{11} kaon decays.

The above di-lepton trigger lines were improved during Run 2 in 2021–2022 as follows. The CHOD and RICH multiplicity conditions have been optimised, leading to a reduction in the trigger rates by a factor of two. The L0 calorimeter trigger has been improved to use the basic cluster topology information. The L1-STRAW trigger algorithm has been enhanced to include vertex reconstruction, track momentum selection, and missing mass reconstruction for online suppression of the $K^+ \to \pi^+\pi^+\pi^-$ background. These developments have allowed a reduction of the downscaling factor of the di-electron trigger line from 8 to 2. The di-electron dataset collected in 2021–2022 is at least a factor of 2 larger than the Run 1 dataset, while the di-muon dataset of 2021–2022 is equivalent to about 80% of the Run 1 dataset.

A new dedicated non-downscaled trigger line was implemented in 2022 to collect tagged neutrino events, i.e. $K^+ \to (\pi^0)\mu^+\nu$ decays followed by charged-current neutrino scattering in the LKr calorimeter. A dataset equivalent to 2×10^{11} fully reconstructed $K^+ \to \mu^+\nu$ decays has been collected with this trigger line so far. While the sample still corresponds to less than one detected tagged neutrino event, a study of control data samples suggests that the signal region is not dominated by backgrounds. We expect to publish the results of the tagged-neutrino analysis in the next year.

In 2022, we published an analysis of the flavour-changing neutral-current decay $K^+ \to \pi^+\mu^+\mu^-$ based on the Run 1 di-muon dataset [5]. The background-free sample obtained of 2.8×10^4 candidates is an order of magnitude larger than the entire previous world sample. The model-independent branching fraction is measured to be $\mathcal{B}_{\pi\mu\mu} = (9.15 \pm 0.08) \times 10^{-8}$, consistent with previous measurements and a factor of three more precise (Figure 7, left). The form-factor parameters in the framework of the Chiral Perturbation Theory (ChPT) at $\mathcal{O}(p^6)$ are found to be $a_+ = -0.575 \pm 0.013$, $b_+ = -0.722 \pm 0.043$, consistent with previous measurements both in the muon and the electron modes (Figure 7, right), and in agreement with lepton flavour universality in $K^+ \to \pi^+\ell^+\ell^-$ decays. The precision of the measurement is limited by the size of the dataset.

We presented a preliminary measurement of the $K^+ \to \pi^+\gamma\gamma$ decay based on the Run 1 minimum-bias dataset at the International Conference on Kaon Physics 2022 [7]. The sample of 4.0×10^3 candidates (with a 10% background) is an order of magnitude larger than the entire previous world sample. The $\hat{c}$ parameter of the ChPT framework at $\mathcal{O}(p^6)$ is measured to be

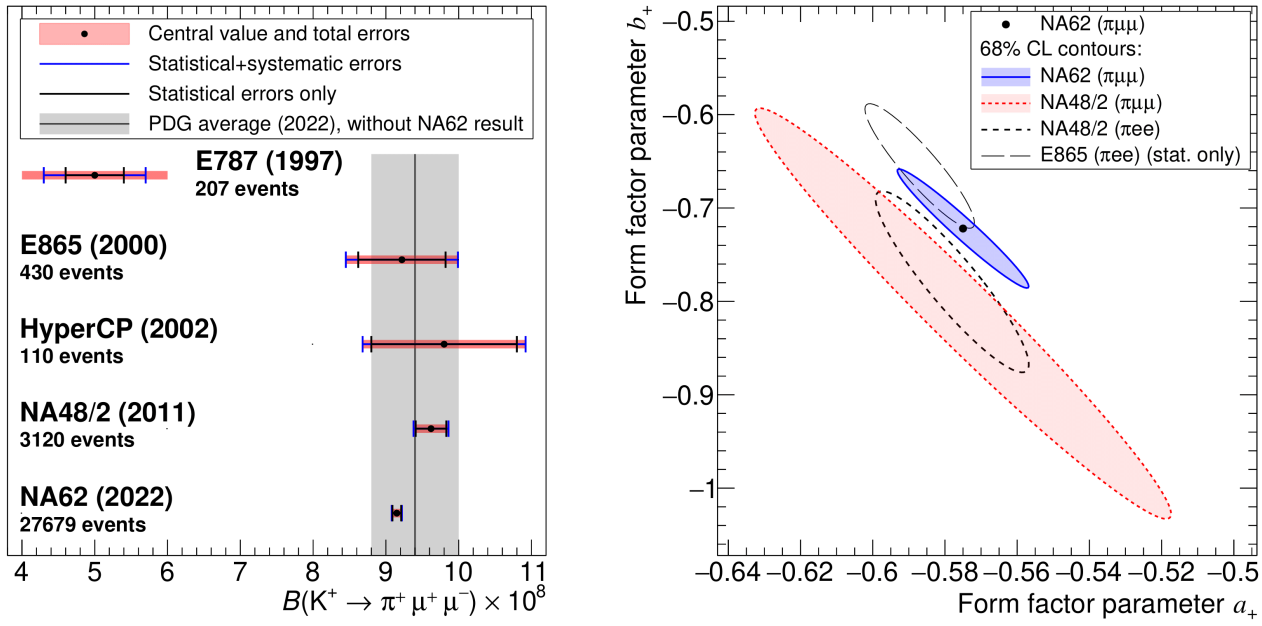

Figure 7: Comparison with earlier measurements. Left: the $K^+ \to \pi^+\mu^+\mu^-$ branching fraction, with the PDG [12] average shown as a shaded band. Right: combined statistical and systematic 68% CL contours in the plane of the form factors (a_+, b_+) for the muon and electron modes.

$\hat{c} = 1.713 \pm 0.084$, and the corresponding branching ratio is found to be $\mathcal{B}_{\pi\gamma\gamma} = (9.73 \pm 0.19) \times 10^{-7}$, a factor of three improvement in precision over previous measurements. A paper, including interpretation of the results in terms of hidden-sector scenarios [13], is in preparation.

A study of the radiative decay $K^+ \to \pi^0 e^+ \nu\gamma$ with the Run 1 minimum-bias dataset has been published as a preprint and submitted to a journal [6]. The decay branching ratio is measured with a percent uncertainty in several restricted kinematic regions, matching the precision of the Chiral Perturbation Theory calculation. In addition, a possible charge asymmetry arising from T-violating effects is investigated and a corresponding upper limit is set.

Ongoing analyses include the measurement of the ratio $\Gamma(K^+ \to e^+\nu)/\Gamma(K^+ \to \mu^+\nu)$, and studies of rare decay modes including $K^+ \to e^+\nu\gamma$, $K^+ \to \pi^+\pi^+\pi^-\gamma$ and $\pi^0 \to e^+e^-$.

Since the submission of the previous annual report to the SPSC, we have published in peer-reviewed journals the following upper limits at 90% CL on lepton flavour or lepton number violating (LFV/LNV) decays based on the full Run 1 dataset [8, 14]:

$$\begin{aligned} \mathcal{B}(K^+ \to \pi^- e^+ e^+) &< 5.3 \times 10^{-11}, \\ \mathcal{B}(K^+ \to \pi^- \pi^0 e^+ e^+) &< 8.5 \times 10^{-10}, \\ \mathcal{B}(K^+ \to \mu^- \nu e^+ e^+) &< 8.1 \times 10^{-11}. \end{aligned}$$

This brings the number of LFV/LNV decay modes of the K^+ and π^0 mesons for which NA62 has set world-leading limits to seven. As the next step towards the completion of the comprehensive LFV/LNV programme with the Run 1 dataset, the first search for $K^+ \to \pi\pi^0\mu e$ decay modes is currently in progress.

The programme of hidden-sector searches in K^+ decays is also in progress. Results to be published shortly include searches for the ultra-rare $K^+ \to \pi^+ e^+ e^+ e^- e^-$ decay, pair-production of hidden-sector mediators in prompt cascades $K^+ \to \pi^+ aa$, $a \to e^+e^-$ and $K^+ \to \pi^+ S$, $S \to A'A'$, $A' \to e^+e^-$, and production of a dark scalar in the process $K^+ \to \pi^+ S$, $S \to \mu^+\mu^-$.

8 Searches for exotic processes

Approximately one week of data was taken in beam-dump mode in October 2021. To minimize the background in this sample, the currents of certain beam-line magnets were adapted to optimize the sweeping of high-energy muons, as described in the last SPSC report.

During this data taking, the intensity of the proton beam dumped on the TAX was just above 150% of the NA62 nominal beam intensity. The total number of protons on dump (POT) is $(1.4 \pm 0.28) \times 10^{17}$. During the past year, major progress on two analyses using this 2021 beam-dump data-set has been achieved:

1. A search for dark photons or axion-like particles decaying to $\mu^+\mu^-$;
2. A search for dark photons decaying to e^+e^-.

Preliminary results from the first analysis were presented at ICHEP 2022. The results were published on arxiv in 2023 [9], and the paper is currently under peer review at JHEP. Preliminary results from the second analysis were presented at La Thuile and Moriond QCD 2023 Conferences.

For both analyses, the signal selection strategy exploits the momentum and vertex reconstruction of the final state leptons. Particle-identification conditions are applied to select $\mu^+\mu^-$ and e^+e^- final states. Finally, the total di-lepton momentum is extrapolated backwards to the point of closest approach to the nominal proton impact points on the TAX: since the signal is produced from proton interactions, it accumulates in a well-defined region in the plane of the distance of closest approach ($\mathrm{CDA_{TAX}}$) vs the longitudinal position of the minimum approach point ($\mathrm{Z_{TAX}}$). For the signal, the two-track invariant mass should peak around the mass of the exotic mediator (dark photon or ALP), with a standard deviation of a few MeV/c^2.

Signal and control regions (SR, CR) for the search of $\mu^+\mu^-$ final states are shown in Figure 8: in the left panel, the observed data (dots) and expected background (colour-scale plot) are superimposed; in the right panel, the observed data (dots) and the expected signal density (colour scale) are superimposed. Both SR and CR were kept blind up to the analysis approval stage. The background, dominated by random pairings of unrelated muons (so-called combinatorial background), was simulated using a data-driven approach. Single muon tracks from an independent trigger line were backward-propagated to a plane preceding the decay-volume. This sample was used as input to a GEANT4-based simulation, to mimic the track overlay and to predict the expected background in the SR. The probability to observe one or more background events in the SR was 1.6% and one event was observed in the signal region (figure 8). There are reasons to suspect that the observed event is of combinatorial origin: the time difference between the two muons is at the level of two signal standard deviations and the observed event is located towards the border of the SR, populated only by the extreme tails of the expected signal distribution. The statistical significance of the observed event corresponds to 2.4σ, not accounting for the shape of the expected signal distribution. The region of the dark photon parameter space (coupling, mass) excluded by the $\mu^+\mu^-$ search is shown in the left panel of Figure 9. The uncertainty on the exclusion is dominated by the uncertainty on the total accumulated POT.

With respect to the $\mu^+\mu^-$ analysis, new optimizations of the decay region, the PID and the signal region were performed for the e^+e^- search. Here, the background is dominated by interactions of the muons with the material traversed producing two mutually in-time tracks (so-called prompt background). A total of $0.0094^{+0.021}_{-0.007}$ background events are expected in the SR, corresponding to a probability of 1.6% of a non-zero observation in the SR. No data event has been observed in the SR. The region of the dark photon parameter space excluded by the e^+e^- search is shown in the right panel of Figure 9.

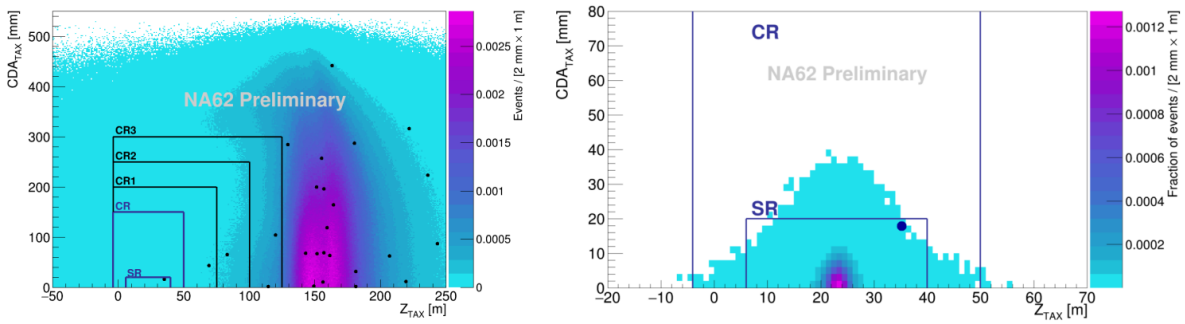

Figure 8: Extrapolation of the total momentum to the production point for $\mu^+\mu^-$ events: closest distance of approach ($\mathrm{CDA_{TAX}}$) vs longitudinal coordinate of the minimum approach point ($\mathrm{Z_{TAX}}$). Data are shown as solid dots. Left: expected background (colour-code plot). Right: expected signal density (colour-code plot).

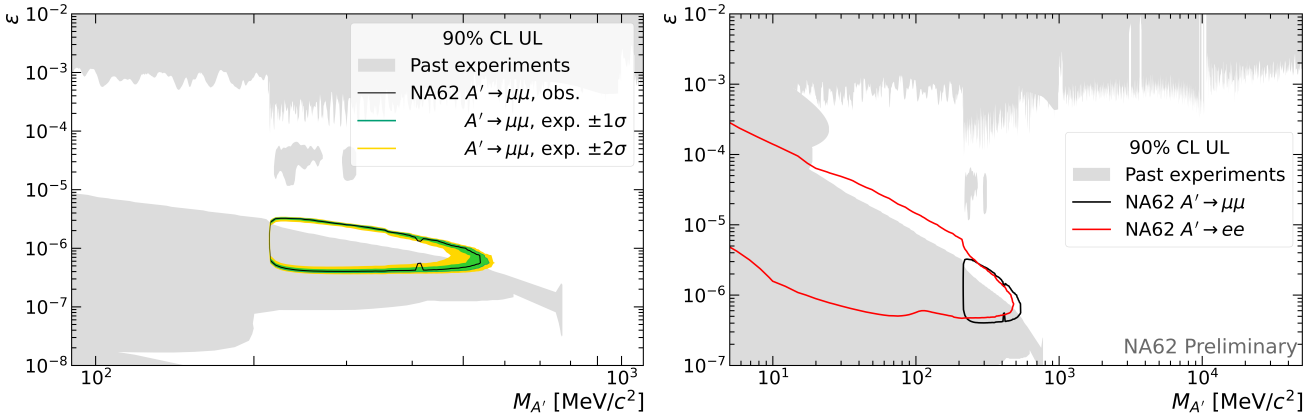

Figure 9: Observed exclusion at 90% confidence level in the dark-photon parameter space (coupling, mass) after the NA62 search for $\mu^+\mu^-$ decays (left) and $\mu^+\mu^-$ and e^+e^- (right) using the 2021 beam-dump data sample. In the left panel, the expected exclusion regions in the absence of a signal shown in green (yellow) colour have 68% (95%) statistical coverage. Regions already excluded by past experiments are shown in grey.

Currently two other analyses that use the 2021 beam-dump sample are on-going, both sensitive to heavy axion-like particles (ALPs) [15]: the search for di-photon ALP decays, and the search for ALPs decaying to $\pi\pi\gamma$ final state. Additional data taking in beam-dump mode is planned for 2023. Such data set will benefit from the significant improvement in the accuracy on the measurement of the number of protons dumped. A campaign of measurements has been performed in 2022 by the beam and radio-protection CERN groups, with the goal of accurately calibrating the beam-intensity monitors through the activation-foil technique. A follow-up study shows that a significant reduction of the uncertainty on the number of dumped protons can be achieved.

9 Publications

Since the last NA62 SPSC review in April 2022, the collaboration has completed the following publications.

- E. Cortina Gil et al. (NA62 collab.), A study of the $K^+ \to \pi^0 e^+ \nu\gamma$ decay, arXiv:2304.12271, submitted to Journal of High Energy Physics [6].
- NA62 collaboration, Search for dark photon decay to $\mu^+\mu^-$ at NA62, arXiv:2303.08666, submitted to Physics Letters B [9].
- E. Cortina Gil et al. (NA62 collab.), A search for $K^+ \to \mu^- \nu e^+ e^-$ decay, Physics Letters B 838 (2022) 137679 [8].
- E. Cortina Gil et al. (NA62 collab.), A measurement of the $K^+ \to \pi^+ \mu^+ \mu^-$ decay, Journal of High Energy Physics, Volume 2022, Issue 11, p.011 [5].
- E. Cortina Gil et al. (NA62 collab.), Improved calorimetric particle identification in NA62 using machine learning techniques, arXiv:2304.10580, submitted to Journal of High Energy Physics [16].
- E. Cortina Gil et al. (NA62 collab.), Performance of the NA62 trigger system, Journal of High Energy Physics, Volume 2023, Issue 03, p.122 [17].

The collaboration is actively contributing to major international conferences and topical workshops with recently published or preliminary physics results from NA62 data analyses. From May 2022 to April 2023, collaboration speakers presented 63 talks at international conferences of which 13 were invited talks, 46 were held in plenary and 17 in parallel sessions. More contributions are already foreseen for the future 2023 conferences.

References

[1] E. Cortina Gil et al. "Measurement of the very rare $K^+ \to \pi^+ \nu\bar{\nu}$ decay". In: *JHEP* 06 (2021), p. 093. DOI: 10.1007/JHEP06(2021)093. arXiv: 2103.15389 [hep-ex].

[2] CERN DG RB 2021 505.

[3] Addendum I to P326, SPSC-2019-039.

[4] 2022 NA62 Status Report to the CERN, SPSC-SR-306.

[5] E. Cortina Gil et al. "A measurement of the $K^+ \to \pi^+\mu^+\mu^-$ decay". In: *JHEP* 11 (2022), p. 011. DOI: 10.1007/JHEP11(2022)011. arXiv: 2209.05076 [hep-ex].

[6] E. Cortina Gil et al. "A study of the $K^+ \to \pi^0 e^+ \nu\gamma$ decay". In: (Apr. 2023). arXiv: 2304.12271 [hep-ex].

[7] A. Shaikhiev (on behalf of NA62). "Study of the rare decay $K^+ \to \pi^+\gamma\gamma$ at the NA62 experiment". https://conference-indico.kek.jp/event/169/contributions/3462/attachments/2345/3018/shaikhiev_KAON22.pdf.

[8] E. Cortina Gil et al. "A search for the $K^+ \to \mu^-\nu e^+ e^+$ decay". In: *Phys. Lett. B* 838 (2023), p. 137679. DOI: 10.1016/j.physletb.2023.137679. arXiv: 2211.04818 [hep-ex].

[9] NA62 Collab., Search for dark photon decays to $\mu^+\mu^-$ at NA62. Mar. 2023. arXiv: 2303.08666 [hep-ex].

[10] EDMS 2621859.

[11] A. Lafuente (CERN), J. Fry, E. Goudzovski (Uni. Birmingham), C. Lazzeroni (Uni. Birmingham), C. Parkinson (Uni. Birmingham), A. Romano (Uni. Birmingham). "A new CEDAR for the NA62 experiment". https://ep-news.web.cern.ch/content/new-cedar-na62-experiment.

[12] R. L. Workman et al. "Review of Particle Physics". In: *PTEP* 2022 (2022), p. 083C01. DOI: 10.1093/ptep/ptac097.

[13] P. Agrawal et al. "Feebly-interacting particles: FIPs 2020 workshop report". In: *Eur. Phys. J. C* 81.11 (2021), p. 1015. DOI: 10.1140/epjc/s10052-021-09703-7. arXiv: 2102.12143 [hep-ph].

[14] E. Cortina Gil et al. "Searches for lepton number violating $K^+ \to \pi^-(\pi^0)e^+e^+$ decays". In: *Phys. Lett. B* 830 (2022), p. 137172. DOI: 10.1016/j.physletb.2022.137172. arXiv: 2202.00331 [hep-ex].

[15] J. Jerhot et al. "ALPINIST: Axion-Like Particles In Numerous Interactions Simulated and Tabulated". In: *JHEP* 07 (2022), p. 094. DOI: 10.1007/JHEP07(2022)094. arXiv: 2201.05170 [hep-ph].

[16] E. Cortina Gil et al. "Improved calorimetric particle identification in NA62 using machine learning techniques". In: (Apr. 2023). arXiv: 2304.10580 [hep-ex].

[17] E. Cortina Gil et al. "Performance of the NA62 trigger system". In: *JHEP* 03 (2023), p. 122. DOI: 10.1007/JHEP03(2023)122. arXiv: 2208.00897 [hep-ex].